The Biological Bulletin, October 2022, volume 243, number 2: 000–000. https://doi.org/10.1086/717565

Reduced Oxygen Impairs Photobehavior in Marine Invertebrate Larvae

LILLIAN R. McCORMICK[1,*], LISA A. LEVIN[1,2], AND NICHOLAS W. OESCH[3,4]

[1]*Integrative Oceanography Division,* [2]*Center for Marine Biodiversity and Conservation, Scripps Institution of Oceanography,* [3]*Department of Psychology, and* [4]*Department of Ophthalmology, University of California–San Diego, La Jolla, California 92093*

Abstract. Organisms in coastal waters experience naturally high oxygen variability and steep oxygen gradients with depth, in addition to ocean deoxygenation. They often undergo diel vertical migration involving a change in irradiance that initiates a visual behavior. Retinal function has been shown to be highly sensitive to oxygen loss; here we assess whether visual behavior (photobehavior) in paralarvae of the squid *Doryteuthis opalescens* and the octopus *Octopus bimaculatus* is affected by low oxygen conditions, using a novel behavioral paradigm. Larvae showed an irradiance-dependent, descending photobehavior after extinction of the light stimulus, measured through the change in vertical position of larvae in the chamber. The magnitude of photobehavior was decreased as oxygen was reduced, and the response was entirely gone at <6.4 kPa partial pressure of oxygen (<74.7 μmol kg^{-1} at 15.3 °C) in *D. opalescens* paralarvae. Oxygen also affected photobehavior in *O. bimaculatus* paralarvae. The mean vertical velocity of paralarvae was unaffected by exposure to reduced oxygen, indicating that oxygen deficits selectively affect vision prior to locomotion. These findings suggest that variable and declining oxygen conditions in coastal upwelling areas and elsewhere will impair photobehavior and likely affect the distribution, migration behavior, and survival of highly visual marine species.

Received 15 March 2021; Accepted 4 October 2021; Published online 26 January 2022.

* To whom correspondence should be addressed. Email: lrmccorm@ucsd.edu.

Abbreviations: GLHT, general linear hypothesis test; GLM, generalized linear model; IR, infrared light; K-W, Kruskal-Wallis; pCO_2, partial pressure of carbon dioxide; pO_2, partial pressure of oxygen.

Introduction

Vision has high oxygen demands, because maintenance of ion gradients needed from photoreceptor and neuronal signaling is energetically expensive (Niven and Laughlin, 2008; Wong-Riley, 2010; Country, 2017). The retina, containing the photoreceptor cells, has one of the highest metabolic demands per gram of tissue in the vertebrate body (Anderson, 1968; Ames, 1992; Waser and Heisler, 2005; Wong-Riley, 2010; Country, 2017). The oxygen demand is especially high in visual structures with high temporal resolution, or fast vision, where signaling must happen at a high rate (Niven and Laughlin, 2008); in the marine environment this occurs in active arthropods, cephalopods, and fish (McCormick and Levin, 2017). The effects of reduced oxygen on vision have been well documented in terrestrial vertebrates and in some fish (Linsenmeier *et al.*, 1983; Johansson *et al.*, 1997). In humans, a reduction in oxygen causes a decrease in absolute sensitivity to light (McFarland and Evans, 1939; Linsenmeier *et al.*, 1983), a decline in color detection (Ernest and Krill, 1971; Vingrys and Garner, 1987), and a decrease in temporal resolution (Fowler *et al.*, 1993). Human eyes are oxygenated through multiple systems of blood vessels to maintain sufficient oxygen at the level of the eye; the outer retina receives oxygen through the choroid vasculature while the inner layers are supported by retinal vasculature (Pournaras *et al.*, 2008). Similarly, some fish have elaborate vasculature (choroid rete) and processes to oxygenate their visual systems (Wittenberg and Wittenberg, 1974; Waser and Heisler, 2005; Damsgaard *et al.*, 2020), and others selectively reduce activity in the visual system as a response to anoxia (Johansson *et al.*, 1997), indicating the high oxygen demands of this system.

In contrast to humans and terrestrial vertebrates, little work has been done to examine the oxygen demands in vision of marine invertebrates, especially larvae, despite the significant

impact that oxygen-impaired vision could have on marine life if responses were similar to what is observed in terrestrial vertebrates (reviewed in McCormick and Levin, 2017). Changes to absolute sensitivity to light can be particularly harmful in the marine environment, because irradiance changes rapidly with depth in the ocean. Cephalopod eyes and vertebrate eyes have many similarities (convergent evolution), and some cephalopods have a partially vascularized circulatory system, with several vessels and associated capillaries directly supplying the eye with oxygen (Young, 1970), which suggests that their eyes have similarly high oxygen demands. Recently, we showed that exposure to reduced oxygen decreases visual signaling at the retinal level in crustacean and cephalopod larvae (McCormick *et al.*, 2019). Here we extend these findings to determine whether impaired retinal activity also changes visual behavior and, thus, might alter the vertical distribution of larvae.

Larvae of many cephalopods, arthropods, and fish rely on vision for a variety of behaviors, including feeding, evading predators, detecting prey, and positioning themselves vertically in the water column (Forward, 1988; Robin *et al.*, 2014). One determinant of vertical distribution in the water column is diel vertical migration (DVM), the daily migration of marine organisms from deeper in the water column during the day to the surface of the ocean at night, and from the surface to depth again at dawn (Forward, 1988; Cohen and Forward, 2009). Diel vertical migration has been documented in larvae of both pelagic and benthic marine invertebrates (Randel and Jékley, 2015), including cephalopods and other highly visual marine organisms (Ambrose, 1981; Zeidberg and Hamner, 2002). For most marine larvae, the cue for migration is primarily light, either a specific irradiance or the detection of a change in light irradiance at a specific rate that initiates phototaxis behavior, causing upward swimming movement toward light (positive phototaxis) or passive sinking or swimming away from light (negative phototaxis) (Rudjakov, 1970; Forward, 1988; Cohen and Forward, 2009). Many marine larvae exhibit another type of photobehavior, where the larvae sink in response to a decrease of irradiance; this has been observed in larvae of marine fish, crustaceans, and at least one cephalopod species (Forward *et al.*, 1996; Charpentier and Cohen, 2015; Puneeta *et al.*, 2018). Here we made use of a robust sinking response at the termination of a light stimulus, which we termed the "OFF-sinking response." The magnitude of this behavioral response was modulated by stimulus irradiance and provided a behavioral readout for visual function. Though not well understood in cephalopod larvae, this response either can be a change in vertical position after a positive phototaxis response or could be a predator shadow response, where larvae sink away from a shadow, indicating a predator, such as a larger fish or ctenophore, moving overhead (Charpentier and Cohen, 2015; Puneeta *et al.*, 2018). Regardless of the reason for the response, this photobehavior relies on detecting a change in irradiance for the cue.

In general, larvae that migrate vertically through the water column must be resilient to very different environmental conditions at the limits of their distribution. Both light and oxygen concentration exhibit strong gradients with water depth in the ocean and high variability over time, particularly on margins with highly productive eastern boundary current upwelling (McCormick and Levin, 2017), fjords (Hansen *et al.*, 2002), tropical gulfs with coastal hypoxia (*e.g.*, Gulf of Mexico, Gulf of California) (Rabalais *et al.*, 2002; Gallo *et al.*, 2020), and shallow bays and estuaries (Tyler *et al.*, 2009). Global ocean deoxygenation has caused the average oxygen content of the ocean to decline by 2% since 1960, and losses can be exacerbated in areas that experience natural variability in oxygen conditions (Schmidtko *et al.*, 2017). In regions such as the Southern California Bight, defined as the coastal region of the eastern Pacific Ocean south of Point Conception and north of the US-Mexico border, where there is high variability in conditions, the partial pressure of oxygen (pO_2) drops quickly from surface waters over the first 300 m of the water column; and low oxygen effects on marine organisms may occur well above the depth of the mid-water, oxygen minimum zone (Gilly *et al.*, 2013). In all of these settings, ongoing climate- and eutrophication-induced ocean deoxygenation threaten to increase the incidence and extent of hypoxia (Breitburg *et al.*, 2018; Kessouri *et al.*, 2021). Similar to oxygen, the irradiance and spectral composition of light also change rapidly with depth in the water column and can vary greatly over time, depending on local conditions (*e.g.*, phytoplankton bloom, *etc.*) (Jerlov, 1951). Both factors are known to limit or influence the distribution of marine organisms (Netburn and Koslow, 2015; Aksnes *et al.*, 2017; Hobbs *et al.*, 2021), but how these two factors interact to impact visual behavior is poorly understood.

Here we provide what we believe are the first measured effects of reduced oxygen on photobehavior in marine invertebrate larvae by using larval cephalopods (called paralarvae) as a model. Vision is critical for their survival (Robin *et al.*, 2014) because feeding must begin immediately upon hatching (Vidal *et al.*, 2002). Cephalopod paralarvae undergo diel vertical migration and have very high metabolic requirements as a result of elevated activity levels and complex visual systems (Pimentel *et al.*, 2012; Vidal *et al.*, 2019); exposure to low pO_2 could significantly impact survival if visual behavior is impaired. We conducted experiments with paralarvae of the market squid, *Doryteuthis opalescens*, and the two-spot octopus, *Octopus bimaculatus*, two cephalopod species common to the Southern California Bight, in order to (1) establish a visual behavior that was modulated by irradiance and use this to (2) examine whether there is oxygen sensitivity of photobehavior in marine larvae and (3) compare results for photobehavior to the oxygen limits for retinal function (McCormick *et al.*, 2019) to determine whether physiological impairment from low oxygen also causes deficits in visual behavior. Based on the decline observed in physiological

retinal function in these species during exposure to reduced oxygen (McCormick *et al.*, 2019), we hypothesized that there would be certain oxygen conditions below which visual behaviors are altered or cease. Our results show that exposure to reduced pO_2 decreased the magnitude of the OFF-sinking response, while locomotor behavior remained unchanged, indicating a selective effect of low oxygen on visual behavior. Based on these results and what other research has shown, we expect deficits in visual behavior to directly translate to altered vertical position in the water column and survivability for paralarvae and suggest that this is a starting point from which to further explore the effects of natural and anthropogenic oxygen variability on behavior in marine animals.

Materials and Methods

Animal collection and rearing

Egg capsules and egg clusters from *Doryteuthis opalescens* (Berry, 1911) and *Octopus bimaculatus* Verrill, 1883 were collected in Monterey Bay and Newport Beach, California, respectively, transported to San Diego, and raised in the laboratory. Paralarvae of *D. opalescens* and *O. bimaculatus* were hatched from capsules and clusters, respectively, kept in a light-controlled experimental room and housed in a 4-L tank with flowing, aerated seawater at a constant temperature of 14 °C under a 13h : 11h light : dark cycle. After hatching, paralarvae were kept in separate 1-L containers at 15 °C with their hatching cohort under the same light cycle, with daily feeding of *Artemia* brine shrimp larvae and/or wild-collected copepods. All paralarvae were tested within one to six days of hatching.

Photobehavior experiments

Photobehavior experiments were conducted 3–11 hours after sunrise, using light stimuli of a range of irradiances during exposure to 4 different oxygen conditions for paralarvae of each species. Swimming behavior was recorded to obtain information about larval position and movement in response to light and to quantify photobehavior.

Experiments were conducted in a vertically oriented, five-sided plexiglass chamber (dimensions: 20 cm H × 5 cm L × 4 cm W) with a removable clear cover, placed in a light-tight enclosure (Fig. 1). Light stimuli were generated by a green

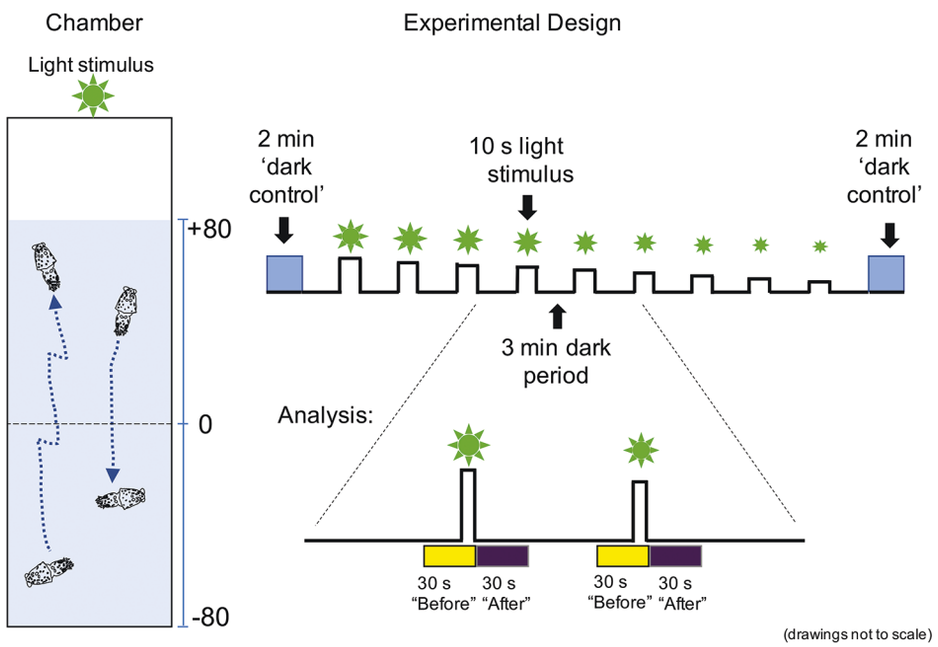

Figure 1. Experimental design for measuring photobehavior of cephalopod larvae. A schematic of the experimental chamber (20 cm H × 4 cm W × 5 cm L) where the behavior of *Doryteuthis opalescens* and *Octopus bimaculatus* paralarvae were measured during exposure to a light stimulus (10-s duration), immediately followed by a 3-min period in darkness. To quantify the larval vertical distribution for analysis, the chamber was numerically described in millimeters, with +80 closest to the light stimulus and −80 as the bottom of the chamber (0 is the center; the chamber was filled to 160 mm). A software program analyzed the tracks of paralarvae (blue dashed lines) during the 30 seconds before termination of the light stimulus (Before; yellow boxes; 20 s dark + 10 s light stimulus) and the darkness 30 seconds after the termination of the light stimulus (After; purple boxes). The analysis was completed for nine irradiance levels and four oxygen conditions to quantify the mean vertical position of the paralarvae and determine the OFF-sinking response. Two 2-minute dark controls were used to measure swimming behavior prior to and after the experiment (blue boxes).

super-bright T-1 3/4 package LED (525 nm; 35 nm full width at half maximum [FWHM]; Thorlabs LED528EHP, Newton, NJ) suspended above the chamber; this wavelength was chosen to match the spectral sensitivity of the larvae (McCormick *et al.*, 2019). Irradiance was controlled using an Arduino Uno microcontroller board and a 16-bit pulse width modulation (PWM) LED driver (Adafruit Industries, New York, NY). The absolute irradiance of the LED was measured using a fiber spectrometer (FLAME-S-VIS-NIR-ES, Ocean Optics, Key Largo, FL) with a cosine corrector (CC-3-UV-S, Ocean Optics), calibrated using a near infrared (NIR)-calibrated lamp (HL-3P-CAL, Ocean Optics). The overhead light passed through a white diffuser filter before reaching the chamber to mimic a natural angular light distribution and prevent abnormal photoresponses that can occur from direct artificial lighting (Forward, 1986). For each experiment, 20 individuals (*D. opalescens*) or 5–6 individuals (*O. bimaculatus*) were added individually into the chamber and tested together. The temperature and pO_2 in the chamber were recorded before and after each trial, using a micro-oxygen sensor and temperature probe (PreSens Precision Sensing, Regensburg, Germany; Microx 4, Pst-7, and St26). With the exception of the light stimuli, experiments were illuminated only with infrared light (IR; >940 nm) for video recording; these wavelengths are outside the sensitivity range of cephalopods (McCormick and Cohen, 2012). Hereafter, illumination with only IR and no visible light is referred to as "dark" or "in darkness." After a 15-minute dark acclimation period, recording started with 2 minutes under only IR illumination for a representation of normal dark behavior (dark control), followed by a series of 9 10-second light stimuli, each followed by a 3-minute dark adaptation period (Fig. 1). The light stimuli decreased in intensity, from 2.45 to 0.063 μmol photons m^{-2} s^{-1}, and the total trial duration was 33 minutes. Experiments were concluded with a second post-experimental dark control to determine whether swimming behavior was different from that during the initial dark control as a result of the experimental design (Fig. 1). Each trial was completed two to four times with different individuals for each of the four different oxygen conditions; water was changed for each trial.

Oxygen treatment

Photobehavior experiments were conducted at four different oxygen conditions for each species, based on previously developed metrics (V_{90}, V_{50}, and V_{10}) for oxygen sensitivity that reflect the pO_2 at which 90%, 50%, and 10% retinal function occurs, respectively, in comparison to normoxia (McCormick *et al.*, 2019). For all experiments, normoxia refers to 100%–105% air saturation and is representative of pO_2 at the ocean surface. For *D. opalescens* paralarvae, the target oxygen conditions tested were normoxia (21 kPa), V_{50} (13 kPa), V_{10} (6.9 kPa), and a low pO_2 (4 kPa), which was a lower pO_2 than V_{10}. Target oxygen conditions for *O. bimaculatus* paralarvae were normoxia (21 kPa), V_{90} (11.5 kPa), V_{50} (7.2 kPa), and V_{10} (5.9 kPa). A custom oxygen and pH control system was used to create all oxygen conditions; this system allowed a change in pO_2 with little change in carbonate chemistry and is a modified version of the system described in Bockmon *et al.* (2013). For all trials, pH was maintained at 8.17 ± 0.12 (SD) for *D. opalescens* paralarvae and 8.12 ± 0.10 (SD) for *O. bimaculatus* paralarvae, which is slightly higher than usual surface pH for this area (~8.07 at 7-m depth), but within normal diurnal variability (±0.10–0.36) (Frieder *et al.*, 2012). The number of trials and the average pO_2, temperature, pH, and larval age for all trials are summarized in Table A1.

Experiment analysis

All trials were recorded under IR illumination using a 2-MP 5–50-mm varifocal lens USB camera (ELP, Shenzhen Ailipu Technology, Shenzhen, China) and saved as a video, using the open-source software Bonsai (Lopes *et al.*, 2015) as an interface. To quantify the photobehavior response, we obtained the position of individual larvae by using EthoVision XT motion-tracking software (ver. 15, Noldus Information Technology, Wageningen, The Netherlands). Results were quantified for each video frame (~60,000 frames for each trial) and then binned into averages for every second throughout the entirety of the experiment for each oxygen condition and species. The mean vertical position of all larvae in the chamber during a trial represents one replicate, which was repeated two to four times per oxygen condition. The averaged vertical position data were boxcar smoothed (10-s average), and mean vertical velocity was calculated from the first derivative of position data over time. Although there are some viscous effects of the walls and the paralarvae experience a moderate Reynolds number (ratio of inertial forces to viscous forces), we do not expect that wall effects will influence the speed or distribution of the larvae because of their relative size and swimming speed (Vogel, 1981; Zakroff *et al.*, 2018).

In order to identify the oxygen sensitivity for photobehavior in *D. opalescens* and *O. bimaculatus* paralarvae, we compared the vertical position of paralarvae in the 30 seconds before the termination of the light stimulus (20 s in dark + 10 s light stimulus: Before) to the vertical position of paralarvae in the 30 seconds after the termination of the light stimulus (After); this was called the OFF-sinking response (Fig. 1). We used a generalized linear model (GLM) examining the effects of the 30-second period (Before/After), oxygen, and irradiance (and the interactions of all three terms) on the mean vertical position of the paralarvae (response term), using a Gaussian distribution and the identity link function ("glm" function in R; R Core Team, 2020). We used the zero-centered means of each Before/After combination for each trial to prevent random changes in vertical position between pairs from affecting significance. Overall statistical significance for terms and interactions was determined by conducting an ANOVA *F* test

on the model. In cases where the 30-second period and oxygen interaction had a significant interactive effect on vertical position, significance between the Before and After vertical position was determined at each oxygen condition, using a general linear hypothesis test (GLHT; "glht" function of the *multcomp* package in R [R Core Team, 2020]; Hothorn *et al.*, 2008) at the mean irradiance (1.19 μmol photons m^{-2} s^{-1}), with the Holm *P* value adjustment method for multiple comparisons. A significant OFF-sinking response is defined here as a significant difference in the mean vertical position of paralarvae between the 30 seconds before the termination of the light stimulus and the 30 seconds after the termination of the light stimulus.

To control for non-visual changes in locomotor behavior attributed to the effects of reduced pO_2 or fatigue, we examined mean vertical velocity of both *D. opalescens* and *O. bimaculatus* as a measure of the swimming ability of the paralarvae. In this analysis, we compared the mean vertical velocity, positive vertical velocity, and negative vertical velocity for both the dark control of normal swimming behavior prior to the start of the experiment and after the conclusion of the experiment (*i.e.*, after all nine light stimuli and dark periods had finished). Kruskal-Wallis (K-W) one-way ANOVA tests were used to determine whether there were differences between the velocity before and after the experiment and whether the velocity was different across oxygen conditions for the mean vertical velocity, positive vertical velocity, and negative vertical velocity.

Unless otherwise stated, all values are given as mean ± 1 standard error of the mean (SEM), significance was considered $P < 0.05$, and "df" denotes degrees of freedom for the given statistical test. All analyses were conducted in R Studio (ver. 1.2.5033), running R (ver. 3.3.3) (R Core Team, 2020).

Results

The first objective was to describe a visual behavior where the vertical position of the paralarvae was modulated in an irradiance-dependent manner. We found strong evidence of a sinking response after termination of the light stimulus in *Doryteuthis opalescens* (Fig. 2A) and limited evidence of a sinking response in *Octopus bimaculatus* paralarvae (Fig. 2B). Importantly, this photobehavior (OFF-sinking response) was modulated by irradiance, with a stronger OFF-sinking response at higher irradiances. *Doryteuthis opalescens* paralarvae showed a significant OFF-sinking response after the termination of the light stimulus (*F* test on GLM, $F = 112.2$, df $= 1, 232$, $P < 0.0001$) (Fig. 3; Table 1) that was affected by irradiance (*F* test on GLM, $F = 7.68$, df $= 1, 244$, $P = 0.006$). *Octopus bimaculatus* paralarvae showed a marginal OFF-sinking response that was affected by irradiance (*F* test on GLM, $F = 17.22$, df $= 1, 134$, $P < 0.001$), but the overall change in vertical position between the 30-second periods was not significant (*F* test on GLM, $F = 1.51$, df $= 1, 142$, $P = 0.222$) (Fig. 4; Table 1). Taken together, these results suggest that the sinking behavior can be a viable experimental paradigm to examine visual behavior in invertebrate paralarvae.

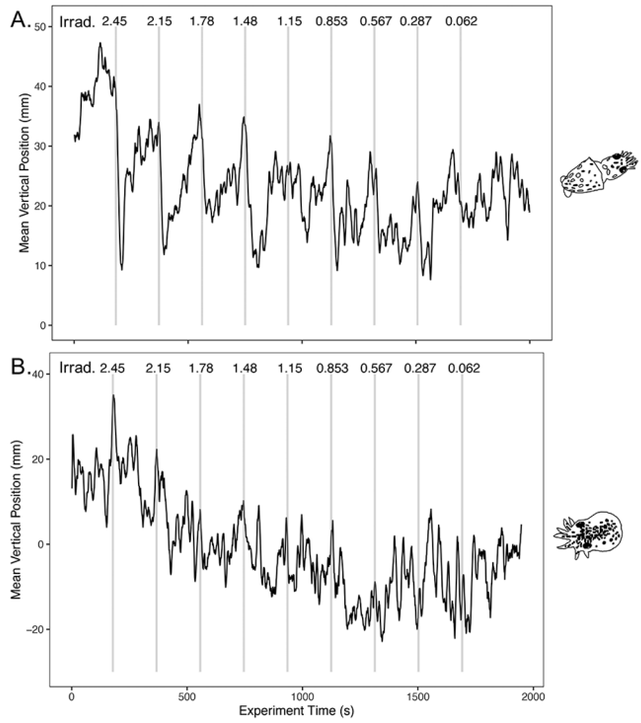

Figure 2. Mean position of larval cephalopods in the photobehavior chamber during the experiment under normoxia showing the OFF-sinking response after termination of the light stimulus. Mean vertical position (mm) of (A) *Doryteuthis opalescens* and (B) *Octopus bimaculatus* paralarvae throughout the experiment (s). Data from all trials in normoxia (21.1–21.3 kPa) were averaged and boxcar smoothed. The 10-second light stimuli are shown as vertical gray bars, with irradiance levels (Irrad.; μmol photons m^{-2} s^{-1}) presented above bars. Chamber is on a scale from 80 (top of the chamber) to −80 (bottom of the chamber), with 0 as the center. Note the difference in vertical scale for the plots.

Oxygen thresholds for photobehavior

Given that vision requires significant metabolic resources, we hypothesized that decreased oxygen partial pressures may specifically impair photobehavior. To test this hypothesis, we repeated these experiments in different oxygen concentrations. In addition to the significant effects of irradiance, we observed that the OFF-sinking response in *D. opalescens* paralarvae was affected by oxygen (*F* test on GLM, $F = 19.86$, df $= 3, 225$, $P < 0.001$) and that the 3-way interaction of 30-second period, oxygen, and irradiance also had a significant effect (*F* test on GLM, $F = 4.25$, df $= 3, 218$, $P = 0.006$) (Table 1). The extent of photobehavior diminished with decreases in both irradiance and oxygen; the OFF-sinking response (decrease in vertical position) was an average of 11.6 ± 1.0 mm in normoxia (21.1 kPa), 6.8 ± 1.4 mm in V_{50} (12.9 kPa), 4.0 ± 1.0 mm in V_{10} (6.4 kPa),

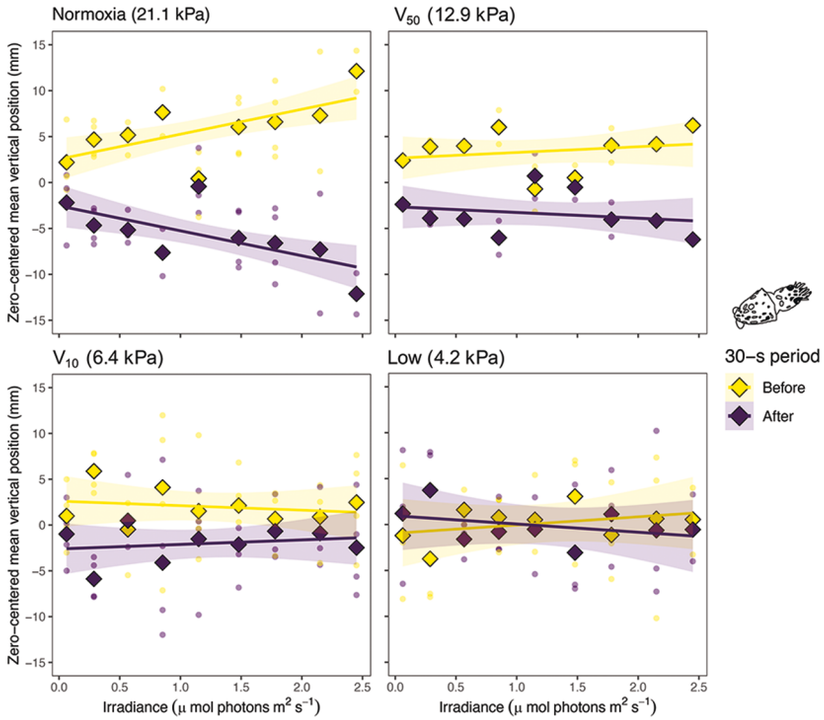

Figure 3. Oxygen effects on photobehavior of *Doryteuthis opalescens* paralarvae in a vertical chamber with an overhead light stimulus. The mean vertical position of paralarvae 30 seconds before the termination of a light stimulus (Before; yellow symbols and lines; 20 s dark + 10-s light stimulus) compared to the mean vertical position of paralarvae 30 seconds after the termination of the light stimulus (After; purple symbols and lines; 30 s dark), centered around zero. Points represent means of individual trials, and diamonds represent the overall mean for each 30-second period. Photobehavior is shown for 4 oxygen levels, normoxia (21.1 kPa), V_{50} (12.9 kPa), V_{10} (6.4 kPa), and low (4.2 kPa), and 9 irradiance levels (μmol photons m^2 s^{-1}). Differences in vertical position between the 30 seconds before and after the termination of the light stimulus, oxygen condition, and irradiance were determined using generalized linear models (GLM); fits and 95% confidence intervals are shown as solid lines and shading, respectively, with colors as described above.

and 0.2 ± 1.2 mm in low oxygen (4.2 kPa) (Figs. 3, A1). *Post hoc* testing showed that this OFF-sinking response was significant in normoxia (GLHT, $Z = 11.59$, $P < 0.001$), V_{50} (GLHT, $Z = 4.77$, $P < 0.001$), and V_{10} (GLHT, $Z = 4.02$, $P = 0.001$) but not under low oxygen (GLHT, $Z = 0.208$, $P = 0.835$) at the mean irradiance level (1.199 μmol photons m^{-2} s^{-1}; Table 2), indicating that while effects on photobehavior were observed at all decreases in oxygen, the absolute oxygen threshold for photobehavior is between 6.4–4.2 kPa (V_{10}-low) for *D. opalescens* paralarvae.

The OFF-sinking response in *O. bimaculatus* paralarvae was also affected by oxygen; the 30-second period × oxygen interaction had a significant effect on vertical position of the paralarvae (F test on GLM, $F = 17.22$, df $= 1, 134$, $P < 0.001$). The 3-way interaction of the 30-second period, oxygen, and irradiance was not significant (F test on GLM, $F = 2.15$, df $= 3, 128$, $P = 0.098$; Fig. 4; Table 1). The OFF-sinking response showed a non-significant decline with a decrease in oxygen and a potential reversal of behavior at the lowest oxygen condition and irradiance levels; paralarvae decreased their vertical position after the termination of the light stimulus by 6.1 ± 2.1 mm in normoxia (21.3 kPa; GLHT, $Z = 2.92$, $P = 0.0956$), 1.5 ± 2.0 mm in V_{90} (10.7 kPa; GLHT, $Z = 0.74$, $P = 1.0$), and 0.7 ± 2.1 mm in V_{50} (7.4 kPa; GLHT, $Z = 0.34$, $P = 1.0$), and increased their vertical position by 3.2 ± 2.1 mm in V_{10} (5.8 kPa; GLHT, $Z = -1.55$, $P = 1.0$) (Table 2; Fig. A2). An oxygen threshold for photobehavior could not be calculated for *O. bimaculatus* paralarvae due to the small sample size per trial (n = 5–6 individuals) and variable behavior of paralarvae.

Oxygen sensitivity of vertical swimming velocity

It is possible that exposure to reduced oxygen could affect processes other than vision, such as locomotion, that could also impair the photobehavior. To test whether this was truly a visual response and not confounded by oxygen effects on swimming capacity, we measured the mean vertical velocity of the paralarvae. The mean vertical velocity was not significantly different in the 2 minutes of darkness at the beginning of the experiment compared to the 2 minutes of darkness (dark controls) at the end of the experiment (K-W, *D.*

Table 1

Results for F *tests (ANOVA) on the generalized linear models (GLM) testing the effects of oxygen and irradiance on vertical position in* Doryteuthis opalescens *and* Octopus bimaculatus *paralarvae*

Species, term and interaction	df	Dev.	Resid. Dev.	*F*	*P* value
D. opalescens					
30-s period	1, 232	2041.61	5423.3	112.20	***<0.001***
O_2	3, 229	0.00	5423.3	0.00	1.000
Irrad	1, 228	0.00	5423.3	0.00	0.999
30-s period:O_2	3, 225	1084.50	4338.8	19.87	***<0.001***
30-s period:Irrad	1, 224	139.89	4198.9	7.69	***0.006***
O_2:Irrad	3, 221	0.00	4198.9	0.00	1.000
30-s period:O_2:Irrad	3, 218	232.24	3966.7	4.25	***0.006***
O. bimaculatus					
30-s period	1, 142	57.94	6227.6	1.51	0.222
O_2	3, 139	0.00	6227.6	0.00	1.000
Irrad	1, 138	0.00	6227.6	0.00	1.000
30-s period:O_2	3, 135	389.55	5838.0	3.37	***0.021***
30-s period:Irrad	1, 134	662.80	5175.2	17.22	***<0.001***
O_2:Irrad	3, 131	0.00	5175.2	0.00	1.000
30-s period:O_2:Irrad	3, 128	248.49	4926.7	2.15	0.097

Photobehavior was measured as a change in the vertical position of paralarvae between the 30 seconds before the termination of the light stimulus compared to the 30 seconds after the termination of the light stimulus (30-s period), for 4 experimental oxygen conditions (O_2), and 9 irradiance levels (Irrad); "df" refers to degrees of freedom, "Dev." refers to deviance, and "Resid." refers to residual. *P* values lower than 0.05 are shown in bold italics.

opalescens: $\chi^2 = 0.014$, df = 1, $P = 0.904$; *O. bimaculatus*: $\chi^2 = 0.0004$, df = 3, $P = 0.983$) or during any of the oxygen conditions (K-W, *D. opalescens*: $\chi^2 = 0.179$, df = 3, $P =$ 098; *O. bimaculatus*: $\chi^2 = 0.521$, df = 3, $P = 0.914$) for either species (Figs. A3, A4).

To examine vertical locomotor activity in finer detail, we separately measured upward (positive) velocity, which requires active swimming in these negatively buoyant paralarvae, and downward (negative) velocity, which represents a passive sinking response. Positive vertical velocity increased with a decrease in oxygen in *D. opalescens* (K-W, $\chi^2 = 41.40$, df = 3, $P <$ 0.001) and was significantly different across oxygen conditions in *O. bimaculatus* (K-W, $\chi^2 = 8.08$, df = 3, $P = 0.044$). Negative vertical velocity also showed an increase in *D. opalescens* paralarvae before and after experiments with a decrease in oxygen (K-W, $\chi^2 = 21.86$, df = 3, $P < 0.001$) and no change in *O. bimaculatus* paralarvae (K-W, $\chi^2 = 7.71$, df = 3, $P = 0.052$). These changes in positive and negative vertical velocity would not cause the decreases in photobehavior observed with oxygen, given that they act opposite to the observed oxygen effects.

Discussion

We demonstrated an irradiance-dependent, robust OFF-sinking response after the termination of a light stimulus in paralarvae of two species. This response decreased under reduced oxygen conditions, and the photobehavior was eliminated at the lowest oxygen levels in *Doryteuthis opalescens* paralarvae. The impairment in photobehavior from reduced pO_2 in *D. opalescens* and *Octopus bimaculatus* could potentially cause paralarvae to miss the visual cue (light) for a change in vertical position, increasing the risk of predation and retention of paralarvae in suboptimal conditions.

Photobehavior in marine larvae

Directed swimming and sinking movements (*e.g.*, photobehavior, geotaxis, chemotaxis, *etc.*) that regulate position in the water column are crucial to the survival of marine larvae. In cephalopod paralarvae, changing position in the water column after hatching moves the paralarvae away from potential predators at the egg site and toward their prey (Fields, 1965; Villaneuva and Norman, 2008) and also enables paralarvae to be transported away from the hatching site by tides and currents (Villaneuva and Norman, 2008; Robin *et al.*, 2014). This has an added benefit of removing paralarvae from potentially stressful (low pO_2, high pCO_2) conditions at the egg bed site (Robin *et al.*, 2014; Navarro *et al.*, 2018). Tidal cues, such as salinity, can be particularly important in controlling vertical distribution for larvae of estuarine animals (Latz and Forward, 1977; Cronin and Forward, 1986). Menhaden larvae (*Brevoortia tyrannus*) show a difference in vertical position when placed in water from offshore *versus* when in estuarine water, likely due to a change in the chemical composition of the water (Forward *et al.*, 1996). In addition, some larvae will actively avoid areas with suboptimal conditions. For example, larvae of the bay anchovy (*Anchoa mitchilli*) and the naked goby (*Gobiosoma bosc*) changed their vertical distribution to avoid oxygen levels <1 mg L^{-1} (Breitburg, 1994). Similarly, in locations where there was a hypoxic bottom in the northern Gulf of Mexico, copepods shifted their distribution to ~7 m shallower than when bottom waters were normoxic

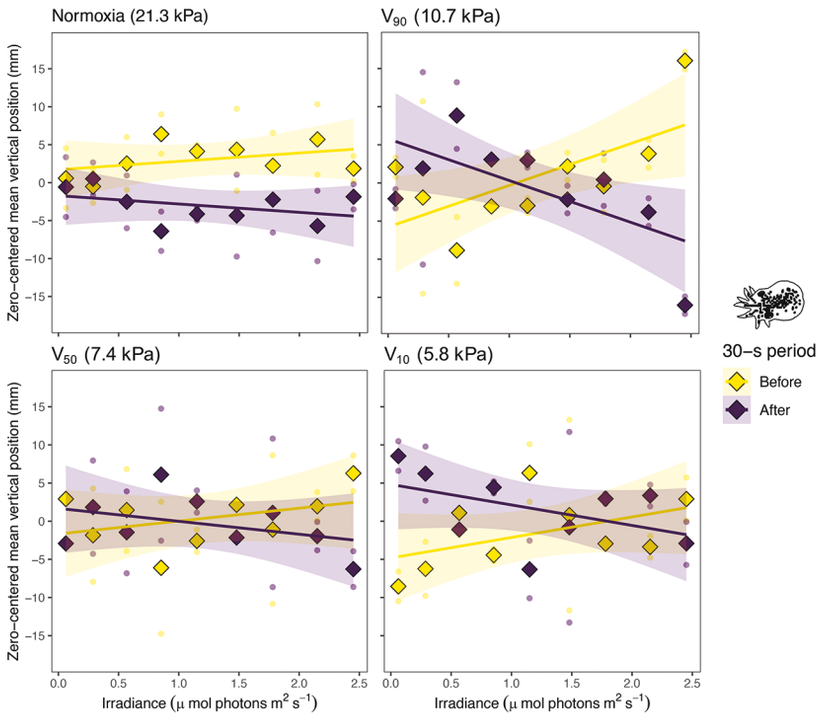

Figure 4. Oxygen effects on photobehavior of *Octopus bimaculatus* paralarvae in a vertical chamber with an overhead light stimulus. The mean vertical position of paralarvae 30 seconds before the termination of a light stimulus (Before; yellow symbols and lines; 20 s dark + 10-s light stimulus) compared to the mean vertical position of paralarvae 30 seconds after the termination of the light stimulus (After; purple symbols and lines; 30 s dark), centered around zero. Points represent means of individual trials (2–4 per oxygen condition), and diamonds represent the overall mean for each 30-second period. Photobehavior is shown for 4 oxygen conditions, normoxia (21.3 kPa), V_{90} (10.7 kPa), V_{50} (7.4 kPa), and V_{10} (5.8 kPa), and 9 irradiance levels (μmol photons m^2 s^{-1}). Differences in vertical position between the 30 seconds before and after the termination of the light stimulus, oxygen condition, and irradiance were determined using generalized linear models (GLM); fits and 95% confidence intervals are shown as solid lines and shading, respectively, with colors as described above.

(Roman *et al.*, 2012). Paralarvae of the ommastrephid squids *Sthenoteuthis oualaniensis* and *Dosidicus gigas* that live in areas with a very shallow oxygen minimum zone in the eastern tropical Pacific (Staaf *et al.*, 2013) are often found concentrated in areas with higher oxygen between the thermocline and the surface (Sánchez-Velasco *et al.*, 2016) and in convergent zones (fronts) (Ruvalcaba-Aroche *et al.*, 2018). The abundance and dispersal of *D. opalescens* paralarvae have been correlated with mesoscale fronts as well as temporal variability in oxygen conditions during El Niño-Southern Oscillation (ENSO) cycles (Zeidberg and Hamner, 2002). Finding an appropriate vertical position in the ocean is critical to survival in marine larvae, and visual impairment from exposure to low oxygen may disrupt the detection of visual cues and change vertical distribution in paralarvae.

The effect of oxygen on photobehavior has been previously demonstrated in only a few studies in marine and aquatic animals. Scherer (1971) found that the negative phototaxis behavior in the walleye fish, *Stizostedion vitreum*, under normoxic conditions was reversed after oxygen was decreased below 1.5 mg O_2 L^{-1} (4.3 kPa at 22 °C). Similarly, normal phototaxis behavior was reversed in adult anemone *Anthopleura elegantissima* and aquatic mayfly larvae *Cloeon dipterum* after exposure to 4.5 mL O_2 L^{-1} (15.4 kPa at 13 °C) and anoxia, respectively (Fredericks, 1976; Nagell, 1977). To our knowledge, this is the first study to determine oxygen effects on photobehavior in cephalopod paralarvae.

The OFF-sinking response observed here is a clear response to light and likely a consistent photobehavior among cephalopod larvae. Cephalopod paralarvae exhibit positive phototaxis; this has been documented in paralarvae of the squids *Todarodes pacificus* (Puneeta *et al.*, 2018), *Doryteuthis* (= *Loligo*) *opalescens* (Arnold, 1965; Fields, 1965), *Loligo forbesii* (Martins, 1997), and octopuses with a paralarval stage (Villaneuva and Norman, 2008), including paralarvae of *O. bimaculatus* (Ambrose, 1981). The sinking response observed here after termination of a light stimulus is similar to the photobehavior described in *T. pacificus* paralarvae, where paralarvae moved to the surface of the experimental tank during a 10-minute light stimulus and then sank after the light was turned off (Puneeta *et al.*, 2018). Here, we extend these results to show the irradiance dependence of the OFF-sinking

Table 2

Results for post hoc *general linear hypothesis tests (GLHT) determining significance in pairwise comparisons of vertical position before and after the termination of a light stimulus in different oxygen conditions in* Doryteuthis opalescens *and* Octopus bimaculatus *paralarvae*

Species, pO_2 level	Estimate (diff)	Standard error	*Z* value	*P* value
D. opalescens				
Normoxia (21.1 kPa)	11.59	1.01	11.53	***<0.001***
V_{50} (12.9 kPa)	6.78	1.42	4.77	***<0.001***
V_{10} (6.4 kPa)	4.04	1.01	4.02	***<0.001***
Low (4.2 kPa)	0.24	1.16	0.21	0.835
O. bimaculatus				
Normoxia (21.3 kPa)	6.05	2.07	2.93	0.096
V_{90} (10.7 kPa)	1.52	2.07	0.74	1.000
V_{50} (7.4 kPa)	0.70	2.07	0.34	1.000
V_{10} (5.8 kPa)	−3.20	2.07	−1.55	1.000

Photobehavior was measured as the difference in the vertical position of paralarvae between the 30 seconds before the termination of the light stimulus compared to the 30 seconds after the termination of the light stimulus (Before – After; "diff"), for 4 experimental oxygen conditions. Comparisons were conducted at the mean irradiance level tested (1.19 μmol photons m^{-2} s^{-1}); V_{90}, V_{50}, and V_{10} refer to the partial pressure of oxygen (pO_2; kPa) corresponding to 90%, 50%, and 10% retinal function as in McCormick *et al.* (2019). "Low" refers to a pO_2 less than V_{10} for *D. opalescens* paralarvae. *P* values lower than 0.05 are shown in bold italics.

response and its utility as a method of quantifying photobehavior that can be used in future studies of cephalopod larvae where measuring phototaxis might be challenging.

The impairment of the OFF-sinking response during exposure to reduced pO_2 in paralarvae of *D. opalescens* and *O. bimaculatus* observed in this study suggests that these larvae will be behaviorally inhibited by exposure to a reduction in pO_2. Paralarvae of both species showed a change in the post-stimulus sinking photobehavior under reduced pO_2, as reflected in the mean position of the larvae in the chamber; the response was stronger for paralarvae of *D. opalescens* than paralarvae of *O. bimaculatus* (Figs. 3, 4). It is reasonable that photobehavior can persist in larvae with some level of retinal impairment, as long as the detection of the change in irradiance is transmitted to the brain. Paralarvae of *D. opalescens* showed an absolute oxygen threshold for photobehavior between 6.4 and 4.2 kPa, where no photoresponse was detected at any irradiance; however, the photobehavior decreased with any reduction in oxygen (Fig. A1). This oxygen threshold corresponds with the oxygen that would cause ~10% retinal function observed in *D. opalescens* paralarvae (McCormick *et al.*, 2019). While there was evidence that oxygen affected photobehavior in *O. bimaculatus* paralarvae, we were not able to calculate an oxygen threshold and compare to the oxygen sensitivity of retinal function. This was likely attributed to the lower sample size of *O. bimaculatus* paralarvae used in each trial (n = 5–6 individuals), in contrast to trials for *D. opalescens* (n = 20 individuals), used to quantify movement and inherent individual variability in behavior. Additional experiments will be necessary to determine the extent of the effect of oxygen on photobehavior for *O. bimaculatus* paralarvae and to determine whether the observed differences are truly species specific. It is also not yet clear whether the decrease in both retinal responses (McCormick *et al.*, 2019), and the subsequent photobehavior, is due to an inability of the vasculature to maintain pO_2 at the level of the eye and brain or whether the decrease is an active suppression mechanism to conserve oxygen in these species (as in Johansson *et al.*, 1997).

Given that oxygen is required for other functions in addition to vision (*e.g.*, swimming), we examined the vertical velocity of paralarvae in darkness to confirm that the behavior observed here was due to visual impairment. We observed no change in the mean vertical velocity of paralarvae of both species in the darkness across oxygen conditions (Figs. A3, A4). When positive and negative vertical velocities were isolated, both species showed a change in vertical velocity that was opposite the response we would expect if oxygen effects on velocity were impacting the visual behavior (Figs. A3, A4). Additionally, other behaviors may affect vertical distributions. For example, cephalopod paralarvae also have strong negative geotaxis (upward swimming behavior) immediately after hatching, but this behavior is reported to lessen with time and be almost diminished after 12 hours post-hatching in *Loligo pealei* (Sidie and Holloway, 1999) and after 2 days in *L. forbesii* (Martins, 1997). Even at one to six days post-hatching we observed a persistent occurrence of negative geotaxis, which led to some paralarvae at the top of the chamber even in the absence of a light stimulus. This, combined with a short-duration stimulus (10 seconds) prevented us from quantifying positive phototaxis in this study, as expected in cephalopod paralarvae (Zeidberg and Hamner, 2002; Villaneuva and Norman, 2008). However, geotaxis was evident at all irradiance levels and oxygen conditions, and it did not compromise the sinking behavior. As a result, we conclude that the OFF-sinking behavior described here was an appropriate method of quantifying photobehavior.

Ecological consequences of impaired photobehavior

Both the ability to detect a change in irradiance and the vertical distribution of larvae can be affected by environmental conditions (Tankersley *et al.*, 1995). The change in photobehavior observed with a decrease in pO_2 in *D. opalescens* and *O. bimaculatus* paralarvae may be exacerbated by other environmental stressors such as carbon dioxide (CO_2), which correlates negatively with oxygen in upwelling areas, such as the Southern California Bight (Frieder *et al.*, 2012; Navarro *et al.*, 2018), and in eutrophic coastal waters (Cai *et al.*, 2011). High variability in both stressors can be observed in the egg development grounds and paralarval habitat for *D. opalescens* and *O. bimaculatus* (Ambrose, 1981; Navarro *et al.*, 2018). Changes in swimming behavior have been observed under high

partial pressure of CO_2 (pCO_2; decrease in pH) in the longfin inshore squid *Doryteuthis pealeii* native to the western Atlantic, with a decrease in the distance traveled, vertical velocity, and mean velocity of day-old paralarvae during exposure to an increase in pCO_2 (Zakroff *et al.*, 2018). If *D. opalescens* paralarvae respond similarly to *D. pealeii*, exposure to both increased pCO_2 and decreased pO_2 could impair swimming velocity and photobehavior, potentially altering distribution even more. Future experiments should consider the interactive effect of these stressors. Additionally, phototaxis is a complicated behavior that employs other sensory modalities in addition to vision, such as extra-ocular photoreception (Ramirez and Oakley, 2015); it is not known the extent to which oxygen or other stressors affect these supporting modalities. Experiments with multiple stimulus exposures (such as both chemical and visual danger cues) could help determine whether oxygen is preferentially used for specific sensory modalities.

The visual sensitivity of cephalopod larvae to oxygen decline is likely to lead to changes in vertical and cross-shore distributions and altered fitness as ocean deoxygenation ensues in coastal waters. Ocean warming is causing reduced solubility and increased stratification, which has led to expansion of oceanic oxygen minimum and oxygen-limited zones (Stramma *et al.*, 2010; Gilly *et al.*, 2013) and has exacerbated eutrophication and coastal hypoxia (Altieri and Gedan, 2015; Breitburg *et al.*, 2018). While we focused on shallow-dwelling cephalopod paralarvae above the oxygen minimum zone, cephalopod or other pelagic marine larvae living in areas where the oxygen minimum zones intersect the coast at very shallow depths (*e.g.*, Mexico, Peru, Chile, the Bay of Bengal, and West Africa) may be especially at risk from the expansion of these zones (Helly and Levin, 2004; Gilly *et al.*, 2013). The Southern California Bight has experienced significant oxygen loss over the past quarter century (Bograd *et al.*, 2015, 2019; Evans *et al.*, 2020; Howard *et al.*, 2020). An oxygen-impaired decrease or cessation of photobehavior may inhibit the ability of larvae to move to areas with sufficient prey items and fewer predators and with the preferred environmental conditions. As larvae move upward to avoid low oxygen or reach better-lighted waters, they may become more vulnerable to predators (Koslow *et al.*, 2011; Netburn and Koslow, 2015). In areas where coastal hypoxia occurs frequently or is increasing as a result of global change (Pitcher *et al.*, 2021), assessments of environmental thresholds and management options should incorporate the oxygen vulnerabilities for vision in highly visual marine larvae.

These results are a crucial first step in determining the effects of environmental oxygen (and other changing conditions) on visual behavior of marine larvae. Additional studies could be completed to determine the oxygen threshold for visual behavior in *O. bimaculatus* paralarvae and/or other pelagic cephalopod larvae. Photobehavior experiments could be completed in a horizontal chamber to remove the effects of geotaxis or focus on other visual behaviors (*e.g.*, prey capture success, camouflage behavior, *etc.*) to expand the results presented here. Future research should focus on holistic methods to test the effects of multiple stressors in addition to oxygen, such as temperature and pH, to further examine the effects of a changing climate on photobehavior in marine larvae or other life stages of vulnerable species. Additionally, the comparison and connection of visual thresholds to other physiological thresholds will be crucial to place oxygen-impaired vision in the context of metabolic and other indices being proposed (Penn *et al.*, 2018; Deutsch *et al.*, 2020; Clarke *et al.*, 2021) to understand the oxygen impacts on marine organisms.

Acknowledgments

We thank W. Gilly, P. Teal, and E. Portner at the Hopkins Marine Laboratory, Stanford University, for providing us with and delivering *Doryteuthis opalescens* egg capsules, and P. Lertvilai and P. Zerofski for obtaining the *Octopus bimaculatus* eggs and zooplankton for feeding the hatched larvae. E. Bockmon was essential to refurbishing the oxygen control system for these experiments, and J. Gonzalez assisted with the setup and design of tanks. We thank E. Peichel, R. Chen, and N. Chan for their tireless efforts on the video processing and J. DiNardo for advice on the statistical analysis. We thank J. H. Cohen for initial discussions on conducting phototaxis experiments and for providing equipment for preliminary experiments. We thank two anonymous reviewers for constructive comments that improved the manuscript. This research was supported by a Philanthropic Educational Organization (P.E.O.). Scholar Award to LRM and National Science Foundation grant OCE-1829623 to LAL and NWO.

Data Accessibility

All data used for this analysis are freely available on the Biological and Chemical Oceanography Data Management Office (BCO-DMO) at https://www.bco-dmo.org/dataset/835968.

Ethical Care Statement

All procedures were in compliance with the Institutional Animal Care and Use Committee (IACUC) of the University of California–San Diego.

Literature Cited

Aksnes, D. L., A. Røstad, S. Kaartvedt, U. Martinez, C. M. Duarte, and X. Irigoien. 2017. Light penetration structures the deep acoustic scattering layers in the global ocean. *Sci. Adv.* **3:** 1–6.

Altieri, A. H., and K. B. Gedan. 2015. Climate change and dead zones. *Glob. Change Biol.* **21:** 1395–1406.

Ambrose, R. F. 1981. Observations on the embryonic development and early post-embryonic behavior of *Octopus bimaculatus* (Mollusca: Cephalopoda). *Veliger* **24:** 139–146.

Ames, A. 1992. Energy requirements of CNS cells as related to their function and to their vulnerability to ischemia: a commentary based on studies on retina. *Can. J. Physiol. Pharmacol.* **70:** 158–164.

Anderson, B. 1968. Ocular effects of changes in oxygen and carbon dioxide tension. *Trans. Am. Ophthalmol. Soc.* **66:** 423–474.

Arnold, J. M. 1965. Normal embryonic stages of the squid, *Loligo pealii* (Lesueur). *Biol. Bull.* **128:** 24–32.

Bockmon, E. E., C. A. Frieder, M. O. Navarro, L. A. White-Kershek, and A. G. Dickson. 2013. Technical note: controlled experimental aquarium system for multi-stressor investigation of carbonate chemistry, oxygen saturation, and temperature. *Biogeosciences* **10:** 5967–5975.

Bograd, S. J., M. P. Buil, E. Di Lorenzo, C. G. Castro, I. D. Schroeder, R. Goericke, C. R. Anderson, C. Benitez-Nelson, and F. A. Whitney. 2015. Changes in source waters to the Southern California Bight. *Deep-Sea Res. Pt. II Top. Stud. Oceanogr.* **112:** 42–52.

Bograd, S. J., I. D. Schroeder, and M. G. Jacox. 2019. A water mass history of the Southern California current system. *Geophys. Res. Lett.* **46:** 6690–6698.

Breitburg, D., L. A. Levin, A. Oschlies, M. Grégoire, F. P. Chavez, D. J. Conley, V. Garçon, D. Gilbert, D. Gutiérrez, K. Isensee *et al.* 2018. Declining oxygen in the global ocean and coastal waters. *Science* **359:** 46.

Breitburg, D. L. 1994. Behavioral response of fish larvae to low dissolved oxygen concentrations in a stratified water column. *Mar. Biol.* **120:** 615–625.

Cai, W., X. Hu, W. Huang, M. C. Murrell, J. C. Lehrter, S. E. Lohrenz, W. Chou, W. Zhai, J. T. Hollibaugh, Y. Wang *et al.* 2011. Acidification of subsurface coastal waters enhanced by eutrophication. *Nat. Geosci.* **4:** 1–5.

Charpentier, C. L., and J. H. Cohen. 2015. Chemical cues from fish heighten visual sensitivity in larval crabs through changes in photoreceptor structure and function. *J. Exp. Biol.* **218:** 3381–3390.

Clarke, T. M., C. C. C. Wabnitz, S. Striegel, T. L. Frölicher, G. Reygondeau, and W. W. L. Cheung. 2021. Aerobic growth index (AGI): an index to understand the impacts of ocean warming and deoxygenation on global marine fisheries resources. *Prog. Oceanogr.* **195:** 102588.

Cohen, J. H., and R. B. Forward, Jr. 2009. Zooplankton diel vertical migration—a review of proximate control. *Oceanogr. Mar. Biol. Annu. Rev.* **47:** 77–110.

Country, M. W. 2017. Retinal metabolism: a comparative look at energetics in the retina. *Brain Res.* **1672:** 50–57.

Cronin, T. W., and R. B. Forward, Jr. 1986. Vertical migration cycles of crab larvae and their role in larval dispersal. *Bull. Mar. Sci.* **39:** 192–201.

Damsgaard, C., H. Lauridsen, T. S. Harter, G. T. Kwan, J. S. Thomsen, A. Funder, C. T. Supuran, M. Tresguerres, P. G. D. Matthews, and C. J. Brauner. 2020. A novel acidification mechanism for greatly enhanced oxygen supply to the fish retina. *Elife* **9:** e58995.

Deutsch, C., J. L. Penn, and B. Seibel. 2020. Metabolic trait diversity shapes marine biogeography. *Nature* **585:** 557–562.

Ernest, J. T., and A. E. Krill. 1971. The effect of hypoxia on visual function: psychophysical studies. *Investig. Ophthalmol. Vis. Sci.* **10:** 323–328.

Evans, N., I. D. Schroeder, M. Pozo Buil, M. G. Jacox, and S. J. Bograd. 2020. Drivers of subsurface deoxygenation in the Southern California Current System. *Geophys. Res. Lett.* **47:** 1–9.

Fields, W. G. 1965. *The Structure, Development, Food Relations, Reproduction, and Life History of the Squid* Loligo opalescens *Berry*, Fish Bulletin 131. State of California Department of Fish and Game.

Forward, R. B., Jr. 1986. A reconsideration of the shadow response of a larval crustacean. *Mar. Freshw. Behav. Physiol.* **12:** 99–113.

Forward, R. B., Jr. 1988. Diel vertical migration—zooplankton photobiology and behavior. *Oceanogr. Mar. Biol.* **26:** 361–393.

Forward, R. B., Jr., J. S. Burkeb, D. Rittschof, and J. M. Welch. 1996. Photoresponses of larval Atlantic menhaden (*Brevoortia tyrannus* Latrobe) in offshore and estuarine waters: implications for transport. *J. Exp. Mar. Biol. Ecol.* **199:** 123–135.

Fowler, B., J. Banner, and J. Pogue. 1993. The slowing of visual processing by hypoxia. *Ergonomics* **36:** 727–735.

Fredericks, C. A. 1976. Oxygen as a limiting factor in phototaxis and in intraclonal spacing of the sea anemone *Anthopleura elegantissima*. *Mar. Biol.* **38:** 25–28.

Frieder, C. A., S. Nam, T. R. Martz, and L. A. Levin. 2012. High temporal and spatial variability of dissolved oxygen and pH in a nearshore California kelp forest. *Biogeosciences* **9:** 1–14.

Gallo, N. D., M. Beckwith, C. L. Wei, L. A. Levin, L. Kuhnz, and J. P. Barry. 2020. Dissolved oxygen and temperature best predict deep-sea fish community structure in the Gulf of California with climate change implications. *Mar. Ecol. Prog. Ser.* **637:** 159–180.

Gilly, W. F., J. M. Beman, S. Y. Litvin, and B. H. Robison. 2013. Oceanographic and biological effects of shoaling of the oxygen minimum zone. *Annu. Rev. Mar. Sci.* **5:** 393–420.

Hansen, B. W., S. Ea, J. K. Petersen, and C. Ellegaard. 2002. Invertebrate re-colonisation in Mariager Fjord (Denmark) after severe hypoxia. I. Zooplankton and settlement. *Ophelia* **56:** 197–213.

Helly, J. J., and L. A. Levin. 2004. Global distribution of naturally occurring marine hypoxia on continental margins. *Deep-Sea Res. Pt. I Oceanogr. Res. Pap.* **51:** 1159–1168.

Hobbs, L., N. S. Banas, J. H. Cohen, F. R. Cottier, J. Berge, and Ø. Varpe. 2021. A marine zooplankton community vertically structured by light across diel to interannual timescales. *Biol. Lett.* **17:** 20200810.

Hothorn, T., F. Bretz, and P. Westfall. 2008. Simultaneous inference in general parametric models. *Biom. J.* **50:** 346–363.

Howard, E. M., J. L. Penn, H. Frenzel, B. A. Seibel, D. Bianchi, L. Renault, F. Kessouri, M. A. Sutula, J. C. McWilliams, and C. Deutsch. 2020. Climate-driven aerobic habitat loss in the California Current System. *Sci. Adv.* **6:** 1–12.

Jerlov, N. G. 1951. Optical studies of ocean water. *Rep. Deep Swed. Exped.* **3:** 1–59.

Johansson, D., G. E. Nilsson, and K. B. Døving. 1997. Anoxic depression of light-evoked potentials in retina and optic tectum of crucian carp. *Neurosci. Lett.* **237:** 73–76.

Kessouri, F., J. C. McWilliams, D. Bianchi, M. Sutula, L. Renault, C. Deutsch, R. A. Feely, K. McLaughlin, M. Ho, E. M. Howard *et al.* 2021. Coastal eutrophication drives acidification, oxygen loss, and ecosystem change in a major oceanic upwelling system. *Proc. Natl. Acad. Sci. U.S.A.* **118:** 1–8.

Koslow, J. A., R. Goericke, A. Lara-Lopez, and W. Watson. 2011. Impact of declining intermediate-water oxygen on deepwater fishes in the California Current. *Mar. Ecol. Prog. Ser.* **436:** 207–218.

Latz, M. I., and R. B. Forward, Jr. 1977. The effect of salinity upon phototaxis and geotaxis in a larval crustacean. *Biol. Bull.* **153:** 163–179.

Linsenmeier, R. A., A. H. Mines, and R. H. Steinberg. 1983. Effects of hypoxia and hypercapnia on the light peak and electroretinogram of the cat. *Invest. Ophthalmol. Vis. Sci.* **24:** 37–46.

Lopes, G., N. Bonacchi, J. Frazão, J. P. Neto, B. V. Atallah, S. Soares, L. Moreira, S. Matias, P. M. Itskov, P. A. Correia *et al.* 2015. Bonsai: an event-based framework for processing and controlling data streams. *Front. Neuroinform.* **9:** 7.

Martins, M. C. P. R. 1997. Biology of pre- and post-hatching stages of *Loligo vulgaris* Lamarck, 1798 and *Loligo forbesi* Steenstrup 1856 (Mollusca, Cephalopoda). Ph.D. dissertation, University of Aberdeen.

McCormick, L. R., and J. H. Cohen. 2012. Pupil light reflex in the Atlantic brief squid, *Lolliguncula brevis*. *J. Exp. Biol.* **215:** 2677–2683.

McCormick, L. R., and L. A. Levin. 2017. Physiological and ecological implications of ocean deoxygenation for vision in marine organisms. *Philos. Trans. R. Soc. A Math. Phys. Eng. Sci.* **375:** 20160322.

McCormick, L. R., L. A. Levin, and N. W. Oesch. 2019. Vision is highly sensitive to oxygen availability in marine invertebrate larvae. *J. Exp. Biol.* **222:** 1–11.

McFarland, R. A., and J. N. Evans. 1939. Alterations in dark adaptation under reduced oxygen tensions. *Am. J. Physiol.* **127:** 37–50.

Nagell, B. 1977. Phototactic and thermotactic responses facilitating survival of *Cloeon dipterum* (Ephemeroptera) larvae under winter anoxia. *Oikos* **29:** 342–347.

Navarro, A. M. O., P. E. Parnell, and L. A. Levin. 2018. Essential market squid (*Doryteuthis opalescens*) embryo habitat: a baseline for anticipated ocean climate change. *J. Shellfish Res.* **37:** 601–614.

Netburn, A. N., and J. A. Koslow. 2015. Dissolved oxygen as a constraint on daytime deep scattering layer depth in the southern California current ecosystem. *Deep-Sea Res. Pt. I Oceanogr. Res. Pap.* **104:** 149–158.

Niven, J. E., and S. B. Laughlin. 2008. Energy limitation as a selective pressure on the evolution of sensory systems. *J. Exp. Biol.* **211:** 1792–1804.

Penn, J. L., C. Deutsch, J. L. Payne, and E. A. Sperling. 2018. Temperature-dependent hypoxia explains biogeography and severity of end-Permian marine mass extinction. *Science* **362:** 1130.

Pimentel, M. S., K. Trubenbach, F. Faleiro, J. Boavida-Portugal, T. Repolho, and R. Rosa. 2012. Impact of ocean warming on the early ontogeny of cephalopods: a metabolic approach. *Mar. Biol.* **159:** 2051–2059.

Pitcher, G. C., A. Aguirre-Velarde, D. Breitburg, J. Cardich, J. Carstensen, D. J. Conley, B. Dewitte, A. Engel, D. Espinoza-Morriberón, G. Flores *et al.* 2021. System controls of coastal and open ocean oxygen depletion. *Prog. Oceanogr.* **197:** 102613.

Pournaras, C. J., E. Rungger-Brändle, C. E. Riva, S. H. Hardarson, and E. Stefansson. 2008. Regulation of retinal blood flow in health and disease. *Prog. Retin. Eye Res.* **27:** 284–330.

Puneeta, P., D. Vijai, J. Yamamoto, and Y. Sakurai. 2018. Orientation patterns of Japanese flying squid *Todarodes pacificus* embryos within egg masses and responses of paralarvae to light. *Zool. Sci.* **35:** 293–298.

R Core Team. 2020. R: a language and environment for statistical computing. [Online]. R Foundation for Statistical Computing, Vienna. Available: https://www.R-project.org [2021, December 3].

Rabalais, N. N., R. E. Turner, and W. J. J. Wiseman. 2002. Gulf of Mexico hypoxia, a.k.a "The Dead Zone." *Annu. Rev. Ecol. Evol. Syst.* **33:** 235–263.

Ramirez, M. D., and T. H. Oakley. 2015. Eye-independent, light-activated chromatophore expansion (LACE) and expression of phototransduction genes in the skin of *Octopus bimaculoides*. *J. Exp. Biol.* **218:** 1513–1520.

Randel, N., and G. Jékely. 2015. Phototaxis and the origin of visual eyes. *Philos. Trans. R. Soc. B Biol. Sci.* **371:** 20150042.

Robin, J., M. Roberts, L. Zeidberg, I. Bloor, A. Rodriguez, F. Briceño, N. Downey, M. Mascaró, M. Navarro, A. Guerra *et al.* 2014. Transitions during cephalopod life history: the role of habitat, environment, functional morphology, and behaviour. *Adv. Mar. Biol.* **67:** 361–437.

Roman, M. R., J. J. Pierson, D. G. Kimmel, W. C. Boicourt, and X. Zhang. 2012. Impacts of hypoxia on zooplankton spatial distributions in the northern Gulf of Mexico. *Estuar. Coasts* **35:** 1261–1269.

Rudjakov, J. A. 1970. The possible causes of diel vertical migrations of planktonic animals. *Mar. Biol.* **6:** 98–105.

Ruvalcaba-Aroche, E. D., L. Sánchez-Velasco, E. Beier, V. M. Godínez, E. D. Barton, and M. R. Pachecho. 2018. Effects of mesoscale structures on the distribution of cephalopod paralarvae in the Gulf of California and adjacent Pacific. *Deep-Sea Res. Pt. I Oceanogr. Res. Pap.* **131:** 62–74.

Sánchez-Velasco, L., E. D. Ruvalcaba-Aroche, E. Beier, V. M. Godínez, E. D. Barton, N. Díaz-Viloria, and M. R. Pachecho. 2016. Paralarvae of the complex *Sthenoteuthis oualaniensis-Dosidicus gigas* (Cephalopoda: Ommastrephidae) in the northern limit of the shallow oxygen minimum zone of the Eastern Tropical Pacific Ocean (April 2012). *J. Geophys. Res. Oceans* **121:** 1998–2015.

Scherer, E. 1971. Effects of oxygen depletion and of carbon dioxide build-up on the photic behavior of the walleye (*Stizostedion vitreum vitreum*). *J. Fish. Res. Board Can.* **28:** 1303–1307.

Schmidtko, S., L. Stramma, and M. Visbeck. 2017. Decline in global oceanic oxygen content during the past five decades. *Nature* **542:** 335–339.

Sidie, J., and B. Holloway. 1999. Geotaxis in the squid hatchling *Loligo pealei*. *Am. Zool.* **39:** 74A.

Staaf, D. J., J. V. Redfern, W. F. Gilly, W. Watson, and L. T. Ballance. 2013. Distribution of ommastrephid paralarvae in the eastern Tropical Pacific. *Fish. Bull.* **111:** 78–89.

Stramma, L., S. Schmidtko, L. A. Levin, and G. C. Johnson. 2010. Ocean oxygen minima expansions and their biological impacts. *Deep-Sea Res. Pt. I Oceanogr. Res. Pap.* **57:** 587–595.

Tankersley, R. A., L. M. Mckelvey, and R. B. Forward, Jr. 1995. Responses of estuarine crab megalopae to pressure, salinity, and light: implications for flood-tide transport. *Mar. Biol.* **122:** 391–400.

Tyler, R. M., D. C. Brady, and T. E. Targett. 2009. Temporal and spatial dynamics of diel-cycling hypoxia in estuarine tributaries. *Estuar. Coasts* **32:** 123–145.

Vidal, E. A. G., M. J. Roberts, and R. S. Martins. 2019. Yolk utilization, metabolism, and growth in reared *Loligo vulgaris reynaudii* paralarvae. *Aquat. Living Resour.* **393:** 385–393.

Vidal, E. A. G., F. P. DiMarco, J. H. Wormuth, and P. G. Lee. 2002. Optimizing rearing conditions of hatchling loliginid squid. *Mar. Biol.* **140:** 117–127.

Villaneuva, R., and M. D. Norman. 2008. Biology of the planktonic stages of benthic octopuses. *Oceanogr. Mar. Biol. Annu. Rev.* **46:** 105–202.

Vingrys, A. J., and L. F. Garner. 1987. The effect of a moderate level of hypoxia on human color vision. *Doc. Ophthalmol.* **66:** 171–185.

Vogel, S. 1981. *The Physical Biology of Flow*. Princeton University Press, Princeton, NJ.

Waser, W., and N. Heisler. 2005. Oxygen delivery to the fish eye: root effect as crucial factor for elevated retinal PO_2. *J. Exp. Biol.* **208:** 4035–4047.

Wittenberg, J. B., and B. A. Wittenberg. 1974. The choroid rete mirabile of the fish eye. I. Oxygen secretion and structure: comparison with the swimbladder rete mirabile. *Biol. Bull.* **146:** 116–136.

Wong-Riley, M. 2010. Energy metabolism of the visual system. *Eye Brain* **2:** 99–116.

Young, J. Z. 1970. Neurovenous tissues in cephalopods. *Philos. Trans. R. Soc. B Biol. Sci.* **257:** 309–321.

Zakroff, C., T. A. Mooney, and C. Wirth. 2018. Ocean acidification responses in paralarval squid swimming behavior using a novel 3D tracking system. *Hydrobiologia* **808:** 83–106.

Zeidberg, L. D., and W. M. Hamner. 2002. Distribution of squid paralarvae, *Loligo opalescens* (Cephalopoda: Myopsida), in the Southern California Bight in the three years following the 1997–1998 El Niño. *Mar. Biol.* **141:** 111–122.

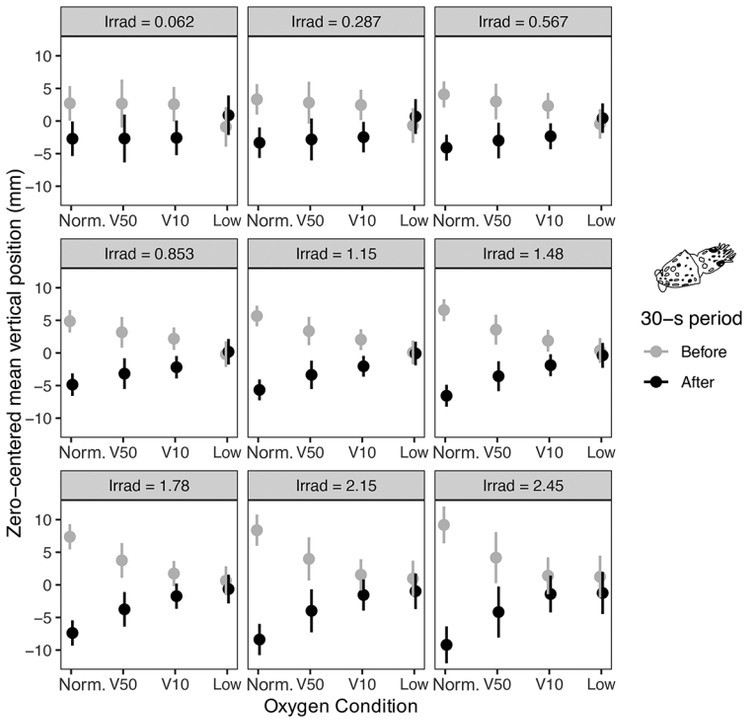

Figure A1. Modeled, zero-centered mean vertical position (mm) of *Doryteuthis opalescens* paralarvae in the 30 seconds prior to the termination of a light stimulus (Before; gray points) and for 30 seconds after the termination of the light stimulus (After; black points) at 4 decreasing oxygen conditions: normoxia (Norm.; 21.1 kPa), V_{50} (V50; 12.9 kPa), V_{10} (V10; 6.4 kPa), and low (4.2 kPa). We used a generalized linear model (GLM) to test the effects of oxygen on the vertical position of *D. opalescens* paralarvae 30 seconds before and after the termination of a light stimulus at 9 different irradiances. Results are shown for each irradiance level (Irrad; μmol photons m^{-2} s^{-1}). Points represent mean values, and error bars represent the standard error around the mean.

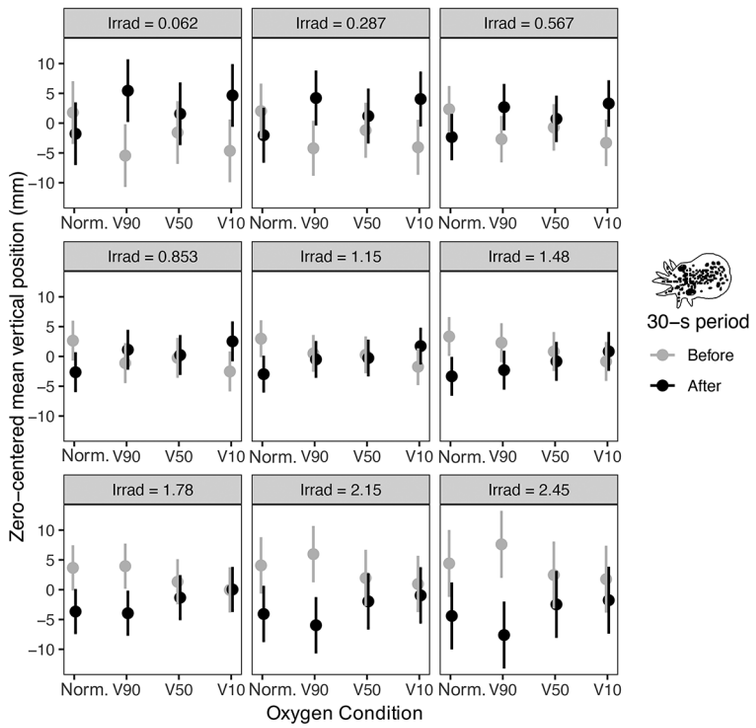

Figure A2. Modeled, zero-centered mean vertical position (mm) of *Octopus bimaculatus* paralarvae in the 30 seconds prior to the termination of a light stimulus (Before; gray points) and for 30 seconds after the termination of the light stimulus (After; black points) at 4 decreasing oxygen conditions: normoxia (Norm.; 21.3 kPa), V_{90} (V90; 10.7 kPa), V_{50} (V50; 7.4 kPa), and V_{10} (V10; 5.8 kPa). We used a generalized linear model (GLM) to test the effects of oxygen on the vertical position of *O. bimaculatus* paralarvae 30 seconds before and after the termination of a light stimulus at 9 different irradiances. Results are shown for each irradiance level (Irrad; μmol photons m^{-2} s^{-1}). Points represent mean values, and error bars represent the standard error around the mean.

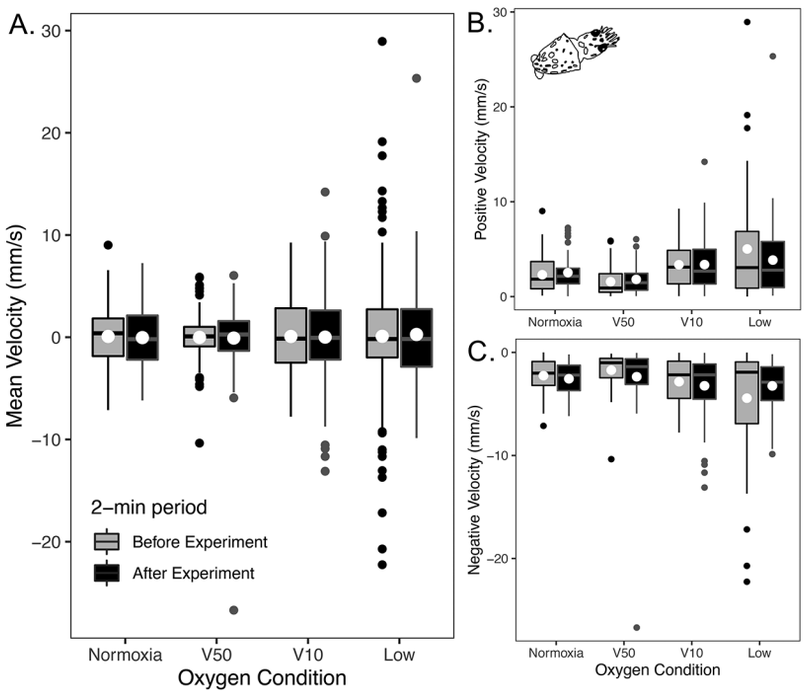

Figure A3. Mean vertical swimming velocity of *Doryteuthis opalescens* paralarvae in darkness before and after photobehavior experiments under four oxygen conditions. (A) Mean vertical velocity (mm s^{-1}), (B) positive vertical velocity (mm s^{-1}), and (C) negative vertical velocity (mm s^{-1}) of paralarvae for a 2-minute period in darkness before the photobehavior experiment started (gray boxes) and a 2-minute period in darkness after the conclusion of the experiment (black boxes) for different experimental oxygen conditions: normoxia (21.1 kPa), V_{50} (12.9 kPa), V_{10} (6.4 kPa), and low (4.2 kPa). Boxes show the median (bold center line) and first and third quartiles of all trials within an oxygen condition; error bars show maximum and minimum values within 1.5× the inner quartile range (IQR = third quartile–first quartile), and solid black points indicate outliers; mean values are indicated with white circles.

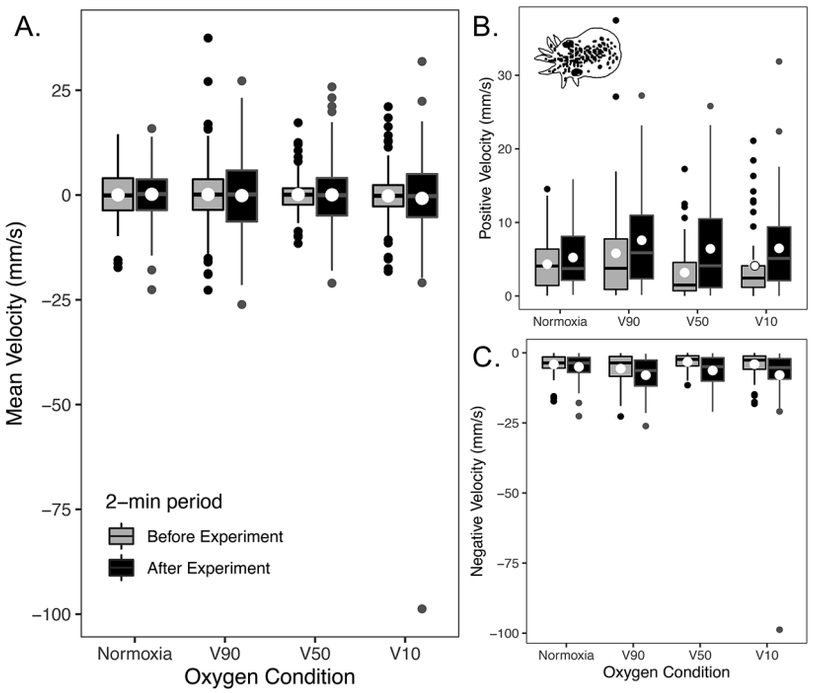

Figure A4. Mean vertical swimming velocity of *Octopus bimaculatus* paralarvae in darkness before and after photobehavior experiments under four oxygen conditions. (A) Mean vertical velocity (mm s^{-1}), (B) positive vertical velocity (mm s^{-1}), and (C) negative vertical velocity (mm s^{-1}) of paralarvae for a 2-minute period in darkness before the photobehavior experiment started (gray boxes) and a 2-minute period in darkness after the conclusion of the experiment (black boxes) for different experimental oxygen conditions: normoxia (21.3 kPa), V_{90} (10.7 kPa), V_{50} (7.4 kPa), and V_{10} (5.8 kPa). Boxes show the median (bold center line) and first and third quartiles of all trials within an oxygen condition; error bars show maximum and minimum values within 1.5× the inner quartile range (IQR = third quartile–first quartile), and solid black points indicate outliers; mean values are indicated with white circles.

Table A1

Description of mean conditions for photobehavior experiments conducted on Doryteuthis opalescens *and* Octopus bimaculatus *paralarvae*

Species	O_2 condition	Mean pO_2 (kPa)	Mean temperature (°C)	Mean pH	Mean age (d)	No. of trials
Doryteuthis opalescens	Normoxia	21.11 ± 0.19	15.80 ± 0.67	8.04 ± 0.01	3.75 ± 1.50	4
	V_{50}	12.90 ± 0.23	14.55 ± 0.28	8.05 ± 0.01	1.0 ± 0.00	2
	V_{10}	6.44 ± 0.35	14.95 ± 0.55	8.27 ± 0.01	4.50 ± 0.58	4
	Low	4.22 ± 0.42	15.65 ± 0.91	8.29 ± 0.01	6.0 ± 0.00	3
Octopus bimaculatus	Normoxia	21.39 ± 0.29	15.87 ± 0.93	8.09 ± 0.09	2.33 ± 1.53	3
	V_{90}	10.72 ± 0.09	15.33 ± 0.39	8.28 ± 0.00	2.0 ± 0.00	2
	V_{50}	7.36 ± 0.47	15.18 ± 0.98	8.08 ± 0.01	2.0 ± 1.41	2
	V_{10}	5.83 ± 0.04	15.73 ± 0.39	8.05 ± 0.04	2.0 ± 0.00	2

Trials were conducted at a variety of ages (days post-hatching [DPH]) and at four different oxygen (O_2) conditions for each species; V_{90}, V_{50}, and V_{10} are oxygen metrics for retinal function derived from McCormick *et al.* (2019). The mean and standard deviation (SD) oxygen partial pressure (pO_2; kPa), temperature (°C), pH, and age are given for each trial.